Optik - International Journal for Light and Electron Optics 205 (2020) 164236

Contents lists available at ScienceDirect

Optik

journal homepage: www.elsevier.com/locate/ijleo

Original research article

Optical, electrical and photoluminescence studies on Al_2O_3 doped PVA capped ZnO nanoparticles for optoelectronic device application

Ravindranadh Koutavarapu[a], R.K.N.R. Manepalli[b], B.T.P. Madhav[c], T. Satyanarayana[d], G. Nagarjuna[e], Jaesool Shim[a,*], M.C. Rao[f,*]

[a] School of Mechanical Engineering, Yeungnam University, Gyeongsan, 712-749, Republic of Korea
[b] Department of Physics, The Hindu College, Machilipatnam, 521001, India
[c] LCRC-R&D, Department of ECE, Koneru Lakshmaiah Education Foundation, Guntur, 522502, India
[d] Department of EIE, Lakireddy Bali Reddy College of Engineering, Mylavaram, 521230, India
[e] Department of Chemistry, S.R.R. & C.V.R. Govt. Degree College, Vijayawada, 520004, India
[f] Department of Physics, Andhra Loyola College, Vijayawada, 520008, India

ARTICLE INFO

Keywords:
ZnO
Co-precipitation
XRD
SEM
Optical
DC conductivity
I-V
PL

ABSTRACT

ZnO is a significant I I-V I n-type direct bandgap semiconductor material which has shown great attention because of its applications in light-transmitting diodes and photograph detectors. In the present investigation, Al_2O_3 doped ZnO nanoparticles were prepared by co-precipitation technique utilizing PVA as a host polymer. X-ray diffraction studies revealed the cubic structure of nanoparticles. The determined normal crystallite size of Al_2O_3 doped PVA capped ZnO nanoparticles was around 12 nm. SEM image showed that the nanoparticles were distributed uniformly with small sized grains consisting of nano dots like tips due to the agglomeration of particles. FTIR demonstrated the trademark vibrational modes of constituent components in the host matrix. The optical studies of all samples displayed close band edge retention at 351 nm (3.26 eV). From the DC studies the conductivity was found to be 3.24×10^{-3} S/cm. EPR studies revealed the crystalline structure and coordination/neighbourhood site evenness of Al_2O_3 doped ZnO in the host lattice. Photoluminescence studies of Al_2O_3 doped PVA capped ZnO nanoparticles demonstrated two groups at 416 and 619 nm. The main band was seen in violet and other band in blue region. These studies revealed that the Al_2O_3 doped PVA capped ZnO nanoparticles materials can be used as LEDs, electroluminescence boards and plasma devices.

1. Introduction

Zinc oxide (ZnO) material possesses a large number of properties when compared to the IV group elements, because of wide energy bandgap of 3.37 eV. It has stable wurtzite structure. When compared to the other materials, ZnO has emerged an attractive material for its different kind of properties and flexible application like reflection coatings, anode materials, solar cells, optoelectronic devices, antibacterial specialist and sensor applications [1,2]. Silicon based transistors are used in many devices. But their energy bandgap is low. In order to fulfil the drawback, ZnO based materials are used as a thin film transistors (TFTs). Owing to its wide energy bandgap and high electrical properties, it is used in optoelectronic and photovoltaic devices. ZnO exhibits high UV

* Corresponding authors.
E-mail addresses: jshim@ynu.ac.kr (J. Shim), raomc72@gmail.com (M.C. Rao).

https://doi.org/10.1016/j.ijleo.2020.164236
Received 2 December 2019; Accepted 16 January 2020

transmitting radiation and gets more stabilized at room temperature, even when compared to the phosphorus and GaN [3]. By using ZnO nanopowders acoustic wave filters which are mostly used in audio and video frequency circuits have been developed [4]. A few creators have announced high photoluminescence efficiencies in ZnO nanostructures [5]. Additionally ZnO is a domain well disposed material, which is uniquely attractive for bio-applications.

Several techniques have been used to prepare the nanomaterials such as spin coating method, CVD technique, thermal decomposition, co-precipitation method etc. Among these co-precipitation method is chosen to prepare the nanoparticles, due to the cost effectiveness as well as the stability in environment conditions such as ambient temperatures, pressure variance etc [6]. Due to these properties, the prepared nanoparticles showed the tremendous change in their size, shapes as well as optical properties. Moreover, the properties can be additionally improved in nano-ZnO structures, nanoparticles, nanowires, which upgrade the exciton oscillator quality and quantum efficiency [7]. In optoelectronic applications, the ZnO particles demonstrated a wide unmistakable photoluminescence in the blue-green locale i.e. 470–550 nm. The obvious outflow is ascribed to deformities, for example, oxygen opening which are accepted to be situated close to the surface region [8]. The properties of ZnO can be customized for spintronic applications however doping diverse progress metal particles such as Co, Al, Mn, V, Fe, etc. into the ZnO lattice. Much exertion has been paid to the natural attractive trade collaborations of ZnO frameworks. So as to address the real instrument of attractive cooperation's in these frameworks, it is similarly critical to have an essential comprehension of various nanoscaled stage development and their outcomes on optical properties [9]. Size consistency and substance dependability in nanosized particles are the primary issues that influence attraction and are stayed to be a test in the field of weakened attractive semiconductors and optoelectronic applications [10].

In this present examination, Al_2O_3 doped PVA capped ZnO nanoparticles were prepared by co-precipitation method. The aim of this work is to prepare the nanosized particles which show a great influence on optoelectronic applications. Until now, based on these aluminium doped ZnO nanoparticles, no proper literature has been found on optoelectronic applications. Due to the insertion of aluminium oxide in the zinc oxide a large number of oxygen vacancies are generated. As a result a wide energy bandgap is obtained. It shows tremendous change on optical properties. The novelty of this present work is to prepare Al_2O_3 doped PVA capped ZnO nanoparticles with cost effective co-precipitation method. The prepared nanomaterials can be used for extensively obtaining the novel materials with different properties, because through this process nanosize grain particles have been deposited with high purity than those reported by other methods. The prepared nanoparticles can give the output which can be utilized in many applications like luminescence, optoelectronic and display devices.

2. Experimental

2.1. Preparation of Al_2O_3 doped PVA capped ZnO nanoparticles

Zinc Oxide (ZnO) and polyvinyl alcohol (PVA) with 98 % purity were obtained from Sigma Aldrich Ltd., India. Cleaned refined water was utilized as a dissolvable. In the present exploratory technique, 50 mL of two fold refined water was taken in a 100 mL of measuring flask. 2.6 g of PVA and 0.050 g of Zinc Oxide were included. The homogenous solution was left for 48 h at room temperature to swell. Later the arrangement was warmed up to 80 °C by steady working as long as 6 h until precipitate was formed. 1.5 mL of sodium hydrogen telluride (NaHTe) and 0.02 mol % nickel oxide were added drop wise to the arrangement. Following couple of minutes a straightforward arrangement was framed. The readied arrangement was thrown on level glass plate dishes and permitted to vanish the dissolvable followed by putting in tourist oven. Al_2O_3 doped PVA capped ZnO nanoparticles were obtained.

2.2. Characterization

XRD pattern was recorded on PANalytical X'Pert Pro X-beam powder diffractometer utilizing CuK_α (1.54060 Å) radiation. Size and morphology of nanoparticles were observed by using Hitachi S-3400 N Scanning electron microscope. FTIR spectrum of the sample was recorded on a Bruker-Alpha FTIR spectrophotometer. The optical transmission spectrum was measured on Hitachi Make UV-VIS spectrometer-3900 in the wavelength range $200-800$ nm. DC conductivity measurement was done by using standard four-probe technique. EPR spectrum of the sample was performed on JEOL JES-FA200 EPR spectrometer. I–V and surface resistance of the prepared nanoparticles were measured using Keithley 2400 Source-Meter. Photoluminescence spectra was recorded on Horiba Jobin-Yvon Fluorolog-3 spectrofluorimeter with Xe continuous (450 W) and pulsed (35 W) lamps as excitation sources. The CIE chromaticity was calculated by using Horiba Jobin-Yvon flouorolog-3 spectrofluorimeter.

3. Results and discussion

3.1. XRD analysis

XRD is utilized to decide the level of crystalline nature of Al_2O_3 doped PVA capped ZnO utilizing Debye-Scherrer's condition. As the particle size increases the intensity of XRD peaks decreases. As a result the FWHM of broadening peaks increases. The low intensity XRD peaks indicate that the films consist of coarsely fine grains (nanocrystalline) and/or are amorphous in nature. The diffraction peaks are observed close to $2\theta = 21.2^\circ$, 38.2°, 42.1° and 53.6° are attributed to (1 1 0), (2 1 1), (3 2 0), and (4 1 0) planes, which are shown in Fig. 1. The obtained peaks are compared to the JCPDS card no. 80-0075. The films are highly oriented along (1 1 0) and (2 0 1) planes. The significant improvement in crystallinity is due to sintering of nanocrystals into effectively larger crystals after the annealed process [11]. The crystalline size data is acquired from FWHM and the normal crystalline size can be determined

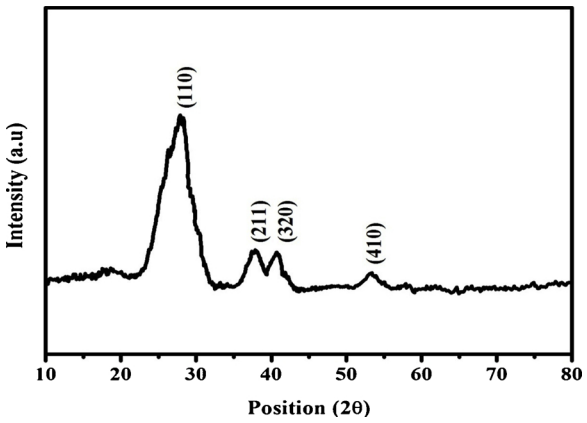

Fig. 1. XRD pattern of Al_2O_3 doped PVA capped ZnO nanoparticles.

by Debye-Scherrer equation.

$$D = (K \lambda / \beta \cos \theta) \quad (1)$$

where

D is the mean crystallite size,
K = 0.9 is Scherrer's constant,
λ is the wavelength of the occurrence pillar,
θ is the diffraction edge,
β is the full width half greatest power of the diffraction top.
From the XRD pattern, the determined estimation of normal crystallite size was 12 nm.

3.2. SEM analysis

Surface morphology and grain size of Al_2O_3 doped PVA capped ZnO nanoparticles were shown in Fig. 2. The prepared nanoparticles were annealed to remove the impurities because the nanoparticles are distributed uniformly with small sized grains consisting of nano dots like tips. This may be due to the agglomeration of particles [12]. At some regions the fusion of agglomerated walls is also observed. The SEM image has been taken at 200 nm resolution. The higher surface harshness is formed due to the capping of PVA polymer and dispersion is plotted at the inset of Fig. 2. The rest of agglomeration of particles are the combination of ZnO doped Al particles which is plotted in the inset of Fig. 2. Figure speaks to the run of the mill SEM micrograph of ZnO-Al nanopowder installed in PVA framework. It has been seen that ZnO-Al nanoparticles like structures lie inside the PVA grid. This micrograph showed that this small concentration of PVA doping in ZnO lattice causes growth of sized grains in some regions which result in porous surface [13]. The bigger ionic radii of aluminium ions distort crystal structure due to ionic radii mismatch which increases grains/particles growth activity of ZnO and formation of bigger particles.

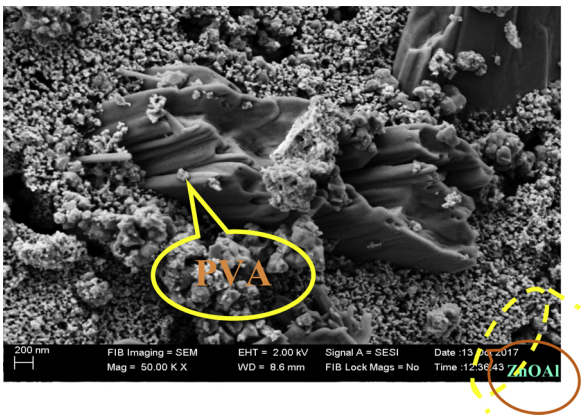

Fig. 2. SEM image of Al_2O_3 doped PVA capped ZnO nanoparticles.

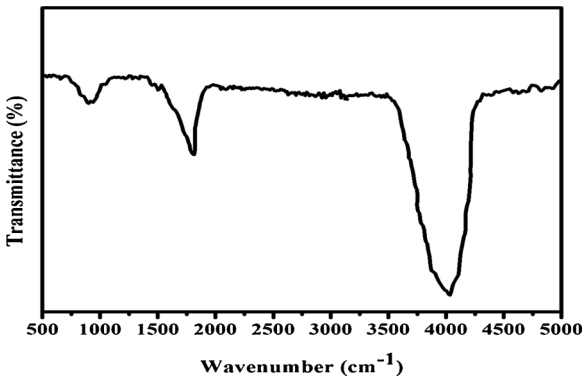

Fig. 3. FTIR spectrum of Al_2O_3 doped PVA capped ZnO nanoparticles.

3.3. FT-IR studies

The characterization peaks of surface useful gatherings of Al_2O_3 doped PVA capped ZnO nanoparticles in the wavenumber range $500-5000\,cm^{-1}$ at room temperature were shown in Fig. 3. The characteristic groups in the FTIR range were formed because of stretching vibrations of Al-O, C═O and C—H, gatherings. The absorption peaks formed at $870\,cm^{-1}$ were expected to C═O extending vibration. The peaks formed at $1700\,cm^{-1}$ were allocated to C—H extending vibration. Moreover, the characteristic peaks of Al-O gatherings were shown at $4800\,cm^{-1}$ viewed as the related aluminium bond among the particles [14]. Hence once again it was confirmed that aluminium oxide decomposes followed by the dissolution of Al^{+} ions within ZnO host lattice by occupying most probably Al^{2+} sites.

3.4. Optical properties

The UV-VIS absorbance spectra in the locale 200–800 nm for Al_2O_3 doped PVA capped ZnO nanoparticles were appeared in Fig. 4. It is obvious from the figure that the assimilation spectrum of the particles is diminished with expanding wavelength. From the figure it is observed that the ingestion expanded with expanding doping convergence of ZnO in PVA matrix [15], as per Beer-lamberts law; the assimilation is corresponding to the quantity of engrossing atoms [16]. Arrangement of new peaks for the sample in the wake of doping and furthermore widening of those peaks with expanding ZnO demonstrate a significant collaboration among PVA and ZnO [17]. This figure shows that the transmittance power increments with the expanding of the wavelength and as the convergence of doped material nano ZnO builds, the transmittance diminishes. The explanation behind this nature is that the increments of grouping of ZnO lead to expanding the limited state of thickness which lessens the transmittance values. The transmission range increments and it is roughly steady at lower absorbance value. It is seen that the composite nanoparticles after doping of aluminium nanoparticles have new peaks were shown in the short wavelengths.

Diffuse reflectance spectrum of prepared nanopowders is shown in Fig. 5. The spectra of all samples display close band edge retention at 351 nm (3.26 eV). Fig. 4 shows the UV–noticeable room temperature optical ingestion spectra of the PVA-ZnO-Al_2O_3 composites. The common place close to band edge ingestion of mass ZnO (3.26 eV) is plainly observed for the sample. It may be seen that the ingestion peaks of the composite containing the bigger size is not standard fit as a fiddle likely because of the arrangement of totals. On account of the particles having size of 200 nm the state of the assimilation peaks are smaller.

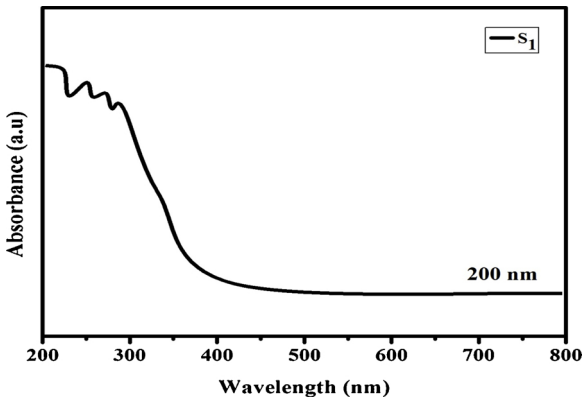

Fig. 4. Optical absorption spectrum of Al_2O_3 doped PVA capped ZnO nanoparticles.

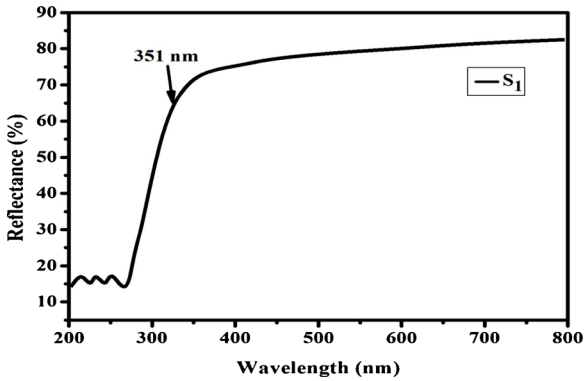

Fig. 5. Reflectance vs wavelength of Al_2O_3 doped PVA capped ZnO nanoparticles.

3.5. DC electrical conductivity studies

The DC electrical conductivity of Al_2O_3 doped PVA capped ZnO nanoparticles were shown in Fig. 6. DC electrical conductivity estimations have been done in the temperature range 200–373 K. The electrical resistivity is calculated by the following equation

$$\rho = \frac{\pi t}{\ln 2}\left(\frac{V}{I}\right) \tag{2}$$

where ρ is the resistivity (Ω-cm), t is the sample thickness (cm), V is the applied voltage and I is the source current (A).

The above plot shows an expansion in conductivity with respect to temperature. This might be because of the hopping mechanism between planning sides, nearby structure unwinding and segmental movement of the polymer. This plot seem to be Arrhenius conduct, with two areas (I & II) with initiation vitality gives above and beneath the dissolving locale 2.9–3.2 K of the polymer. In locale I, the conductivity increments gradually while in area II, it increments at higher rate. The last might be because of the adjustment in stage from a semi- crystalline to an indistinct state at the dissolving point. Further the shapeless area dynamically increments in district II because of which polymer chain gains quicker inward modes for which bond pivot produce segmental movement. This favours bouncing of particles with in the middle of the chains and thus the conductivity turns out to be high [18]. Comparable reports have likewise been accounted for electrolytes dependent on PVA.

The temperature reliance of the DC resistivity can be shown by the outstanding Arrhenius condition. Micheletti and Mark evaluated the intergranular boundary stature (φ_b) from the accompanying condition:

$$\mu = \mu_0 \exp(-\varphi_b/KT) \tag{3}$$

where each one of the terms have their typical implications. The estimation of (φ_b) acquired from plot Fig. 6, log (ρ) versus $1/T$ is 0.61 eV. Charge bearer versatility μ is resolved from the relation given by

$$\mu = \sigma/ne \tag{4}$$

Where n is electron thickness and σ is the conductivity. It infers the semiconducting idea of the example since conductivity increments with increment in working temperature because of increasing of transport of ions. From the plot the calculated conductivity was found to be at 3.24×10^{-3} S/cm. The expansion conductivity with increment of temperature demonstrates total undefined stage and is like similar in daintily doped PVA film. It was recommended that a variable range jumping conduction model can be applied for

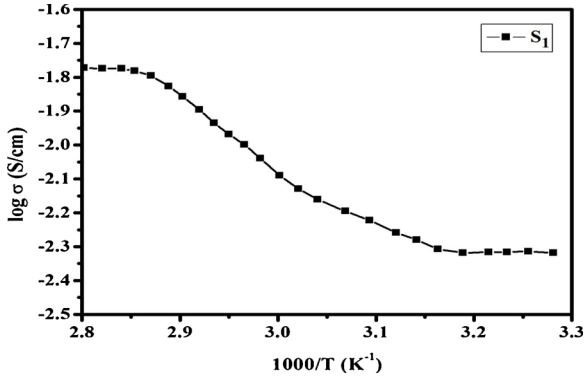

Fig. 6. DC conductivity of Al_2O_3 doped PVA capped ZnO nanoparticles.

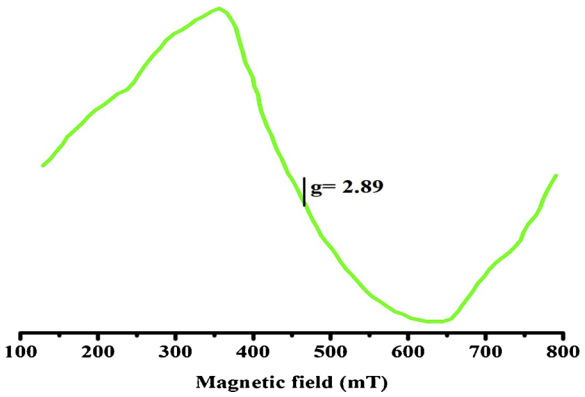

Fig. 7. EPR spectrum of Al_2O_3 doped PVA capped ZnO nanoparticles.

such situation where the conductivity is estimated.

3.6. EPR studies

EPR spectrum of Al_2O_3 doped PVA capped ZnO nanoparticles were measured on JEOL JES-FA200 having 100 kHz field regulation at room temperature was shown in Fig. 7. The reverberation sign was determined at g = 2.89 for 100 K temperature. The variation in the magnetic field was observed due to the insertion of Al^+ ions in the ZnO crystal lattice. The insertion of Al^+ ions in a host polymer induced the magnetic behaviour in the ZnO nanoparticles and also exhibit ferromagnetic nature at room temperature [19]. The Al_2O_3 doping may change the perfect ZnO structure to make it possible for forming defects and holes which could be regarded as additional charge carriers. It was clear that Al^+ (d6) particles have octahedral coordination and orbital singlet $^3A_{2g}$ has the most reduced vitality level, which split in to 3 F ground state as an outcome of crystal field. Turn Hamiltonian is utilized to speak to the EPR range of Al^+ particle for an isotropic g factor. An isotropic line is acquired which relates to the |0–1' |±1' attractive dipole changes. The turn - Hamiltonian can be represented as,

$$H = g\beta BS + SAI + SDS \quad (5)$$

where g is the isotropic factor,
β is the Bohr magnetron,
B is the external magnetic field,
S is the vector operator of the electron spin momentum,
A is the hyperfine interaction parameter,
I is the vector operator of nuclear spin momentum,
and D is the zero field splitting parameter.

From the above relations the accompanying parameters can be determined. The isotropic factor 'g' esteem is 2.89. The Δ worth is 9532 cm^{-1} in the wavelength of λ = 353 cm^{-1}. The communication with the electric field segment of the proper recurrence of electromagnetic radiation can start a change between the two states and results in the assimilation of photons. The fundamental rule in the EPR method is the ingestion of concoction substance in the vitality levels, which may reach out over a wide wavelength run in an outer attractive field. By EPR and UV-noticeable investigations the ionic parameter, α^2 can be assessed by,

$$g = 2.0023 - (\alpha^2 8\lambda/\Delta) \quad (6)$$

The ionic parameter lies in the middle of 0.2 and 1.5 which means the readied nanoparticles contain ionic and covalent holding. The acquired ionic parameter estimation of α^2 is 0.84. This unequivocally recommends that there exists a covalent holding between doped Al^+ particles and its ligands presence in the host lattice [20].

3.7. I–V characteristics

I–V characteristics of the prepared nanoparticles were shown in Fig. 8. The basic principle includes in I–V qualities is the charge move of electrons upgrade through the doped sample. Consequently the ionic conduction happens in the sample. Al^+ doped particles get quickly circulated over the stick gaps in the sample. At the point when the temperature of the sample should be brought up in the conduction phenomenon, at that point the charge transport is conceivable through the nanoparticles in the host material [21]. From the obtained plot, it clearly shows that the prepared nanoparticles possess the semi-conduction behaviour. Fig. 8 plainly demonstrates the voltage required for current and is obtained above the + ve side indicates the bright light. It is obvious that the voltage necessary for current is obtained below the + ve side indicates the dark light [22]. It is also obviously clear that the Al_2O_3 doped PVA capped ZnO nanoparticles, is a perfect material which is utilized for semiconducting applications. The dull current in the turnaround inclination is exceptionally close to zero and it could be considered a perfect case for diode qualities.

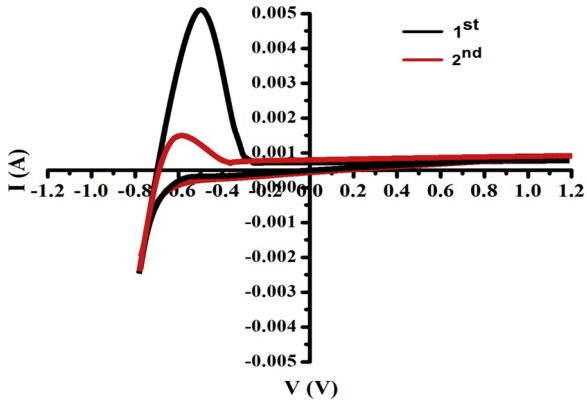

Fig. 8. Current- voltage characteristics of Al_2O_3 doped PVA capped ZnO nanoparticles.

3.8. Photoluminescence studies

The photoluminescence spectrum of Al_2O_3 doped PVA capped ZnO was shown in Fig. 9. Blue emission states are attributed to surface defects. These are hidden in the crystalline surface, whereas the bond formation and their respective boundaries are additionally perceived. Band twisting will bring about formation of a consumption district at the grain limits and it will influence the ionization condition of the deformities inside the exhaustion locale. Since the annealed sample comprises of fine particles with an enormous surface territory and bunches of grain limits, the green outflow likely to begin from contributor acceptor changes, where benefactor and additionally acceptor imperfections are situated at surfaces or grain limits [23,24]. From the figure, it is seen that, annealed sample has showed two excitation peaks at 416 and 619 nm. Everything happens because of excitation wavelength of 353 nm at room temperature. The acquired groups demonstrate the shading organized in the unmistakable district and furthermore the locale demonstrates that the main band is seen in violet area and the subsequent band in blue locale [25]. In this way the readied nanoparticles are valuable in the showcase gadget applications.

CIE color chromaticity is framed by the interesting combination of three coordinates which are green, blue and red with proper proportions. The light emission radiated by Xe source has monochromatic wavelength which is incident on the sample. The yield of the sample blower recognizes the approaching radiation. The subsequent radiation is sifted by an outflow monochromator which results in to a sign of a photomultiplier identifier [26]. CIE 1931 chromaticity directions are observed to be at x = 0.2053 and y = 0.1453. The related CIE outline is appeared in Fig. 10. The CIE chromaticity, organized locale for the readied nanoparticles is found in blue region.

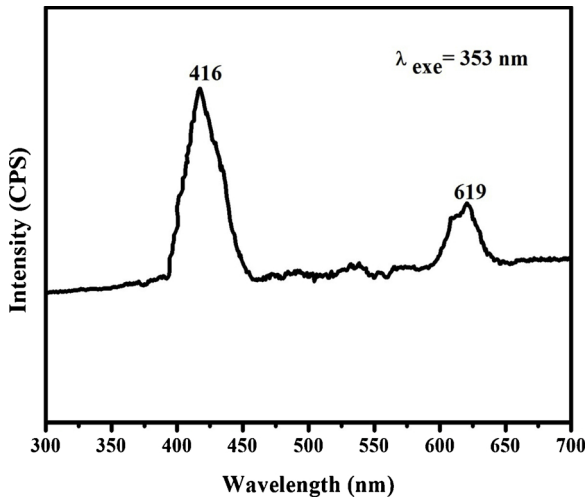

Fig. 9. Photoluminescence spectrum of Al_2O_3 doped PVA capped ZnO nanoparticles.

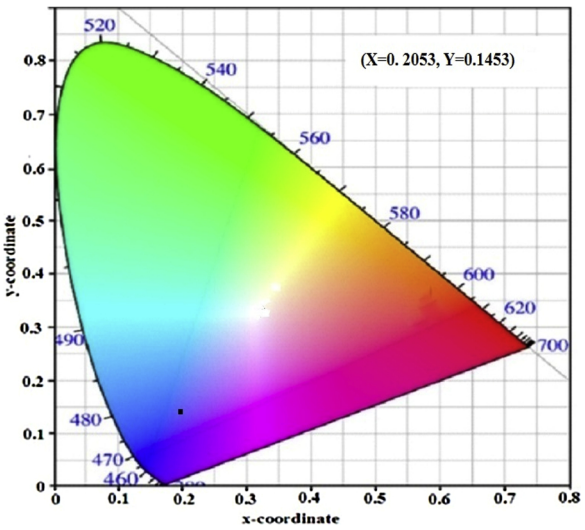

Fig. 10. Chromaticity diagram of Al_2O_3 doped PVA capped ZnO nanoparticles.

4. Conclusions

Al_2O_3 doped PVA dopped ZnO nanoparticles were obtained by co-precipitation method. From the XRD pattern, the diffraction peaks observed close to $2\theta = 21.2^{\circ}$, 38.2°, 42.1°, and 53.6° were attributed to the (1 1 0), (2 1 1), (3 2 0), and (4 1 0) planes. The normal crystallite size was 12 nm. SEM image showed that the nanoparticles are distributed uniformly with small sized grains consisting of nano dots like tips due to the agglomeration of particles. The characteristic groups in the FTIR range were formed due to stretching vibrations of Al-O, C═O and C−H, gatherings. The absorption peaks formed at 870 cm^{-1} were expected to C═O extending vibration. The optical spectrum of all examples displays close band edge retention at 351 nm (3.26 eV). From the DC plot the calculated conductivity was found to be at 3.24×10^{-3} S/cm. The expansion in conductivity with increment of temperature demonstrates total undefined stage and is like similar in daintily doped PVA film. The voltage required for current was obtained above the + ve side indicated as bright light and the voltage below the + ve side indicated as dark light. Photoluminescence studies revealed that the annealed sample have showed two excitation peaks at 416 and 619 nm. CIE chromaticity of the readied nanoparticles was found in blue region. These studies revealed that the prepared nanoparticles can be utilized in many applications like luminescence, optoelectronic and display devices.

Role of the funding sources

There are no funding sources for this article work.

Declaration of Competing Interest

The authors declare that there is no conflict of interest regarding the publication of this paper.

References

[1] A. Van Dijken, E.A. Meulenkamp, D. Vanmaekelbergh, A. Meijerink, J. Lumin. 454 (2000) 87–89.
[2] I. Shalish, H. Temkin, V. Narayananmurti, Phys. Rev. B 69 (2004) 245401.
[3] M. Ghosh, A.K. Raychaudhuri, Appl. Phys. Lett. 93 (2008) 123113.
[4] S. Deka, P.A. Joy, Solid State Commun. 142 (2007) 190–194.
[5] A. Debernardi, M. Fanciulli, Physica B 401–402 (2007) 451–453.
[6] A.J. Chen, X.M. Wu, Z.D. Sha, L.J. Zhug, Y.D. Meng, J. Phys. D 39 (2006) 4762.
[7] Y.Q. Wang, S.L. Yuan, P. Liu, X.X. Lan, Z.M. Tian, J.H. He, S.Y. Yin, J. Magn. Magn. Mater. 320 (2008) 1423–1426.
[8] S. Bachiv, C. Sandouly, J. Kossanyi, J.C. Ranford-Haret, J. Phys. Chem. Solids 57 (1996) 1869–1879.
[9] M. Naeem, S.K. Hasanain, M. Kobayashi, Y. Ishida, A. Fujimori, S. Buzby, S.I. Shah, Nanotech 17 (2006) 2675–2680.
[10] M. Naeem, S.K. Hasanain, A. Mumtaz, J. Phys. Condens. Mater 20 (2008) 025210.
[11] A.K. Srivastava, M. Deepa, N. Bahadur, M.S. Goyat, Mater. Chem. Phys. 114 (2009) 194–198.
[12] N. Bouropoulos, G.C. Psarras, N. Moustakas, A. Chrissanthopoulos, S. Baskoutas, Phys Stat Sol 205 (2008) 2033–2037.
[13] J. Lee, E.M. Bourim, W. Lee, J. Park, M. Jo, S. Jung, J. Shin, H. Hwang, Appl. Phys. Lett. 97 (2010) 172105.
[14] R. Viswanatha, S. Sapra, S.S. Gupta, B.B. Satpati, P.V. Satyam, B.N. Dev, D.D. Sarma, J. Phys. Chem. B 108 (2004) 6303–6310.
[15] A.S. Roy, S. Gupta, S. Sidhu, A. Praveen, C. Ramamurthy, Compos. Part B Eng. 47 (2013) 314–319.
[16] A. Wasan, T. Mohammed, K. Tagreed, J. Baghdad Sci. 8 (2011) 543–550.

[17] M. Hamed, H. Sabah, A. Sarkawt, Asian Trans. Sci. Tech. 1 (2012) 16–20.
[18] A. Kurt, Turkish J. Chem. 34 (2010) 67–79.
[19] J. Antony, S. Pendyala, D.E. McCready, M.H. Engelhard, D. Meyer, A. Sharma, Y. Qiang, IEEE Trans. Magn. 42 (2006) 2697–2699.
[20] Y.Y. Tay, S. Li, C.Q. Sun, P. Chen, Appl. Phys. Lett. 88 (2006) 173118.
[21] K.J. Albert, N.G. Lewis, C.L. Sahauer, G.A. Sotzing, S.E. Stizel, T.P. Vaid, D.R. Walt, Chem. Rev. 100 (2000) 2595–2626.
[22] B. Ashkenov, N. Mbenkum, C. Bundesmann, V. Riede, M. Lorenz, D. Spemann, M. Kaidashev, A. Kasic, M. Schubert, M. Grundmann, G. Wagner, H. Neumann, V. Darakchieva, H. Arwin, B. Monemar, J. Appl. Phys. 93 (2003) 126–133.
[23] G. Xiong, U. Pal, J.D. Serrano, J. Appl. Phys. 101 (2007) 024317.
[24] F. Decremps, J.P. Porres, A.M. Saitta, J.C. Chervin, A. Polian, Phys. Rev. B 65 (2002) 092101.
[25] V.A. Fonoberov, A.A. Balandin, Phys. Rev. B 70 (2004) 233205.
[26] J. Yang, X. Liu, L. Yang, Y. Wang, Y. Zhang, L. Lang, M. Gao, B. Feng, J. Alloys Compd. 477 (2009) 632–635.